

HOLOGRAPHIC STUDY
OF
ELECTRICAL RESPONSE OF BONE

THESIS

Presented to the Graduate Council of
Southwest Texas State University
in Partial Fulfillment of
the Requirements

For the Degree of

MASTER OF SCIENCE

By

Tony Castillo, B. S.
(San Marcos, Texas)

December, 1974

ACKNOWLEDGEMENTS

The author would like to express his gratitude to Dr. James R. Crawford, graduate advisor and Assistant Professor of Physics, for his time, patience, and guidance. Appreciation is expressed also to the graduate committee members, Dr. Victor E. Michalk, Associate Professor of Physics, Mr. Arthur W. Spear, Associate Professor of Physics, and Dr. Lynn H. Tulloch, Professor of Mathematics, for their assistance.

Likewise, the author thanks John Pasquali and the computer center personnel at Southwest Texas State University for their timeless efforts in the construction of the fortran program presented.

Tony Castillo

December, 1974

San Marcos, Texas

TABLE OF CONTENTS

Chapter	Page
LIST OF FIGURES	v
LIST OF TABLES	vi
I. INTRODUCTION	1
II. EXPERIMENTAL DESCRIPTION	5
A. Bone Sample Preparation	5
B. Experimental Arrangement	6
C. Holographic Analysis	10
III. EXPERIMENTAL DISCUSSION	17
A. Electrical Response of Bone	17
1. Holographic interferometry applied to elec- trically stressed bone	
2. Dependence of displacement on electric field strength	
IV. CONCLUSION	41
APPENDIX	42
REFERENCES	55

LIST OF FIGURES

	Page
Figure 1. Arrangement of laser and components	8
Figure 2. Pure translation of a surface	12
Figure 3. Points of observation where observer is normal to hologram plate	19
Figure 4. Geometrical lay-out for observations	21
Figure 5. Photograph of an illuminated hologram	32
Figure 6. Plot of logarithms of the displacement versus the magnitude of the applied voltage	39

LIST OF TABLES

Table	Page
I. Data for Calculated Displacement of Plastic	24
II. Calculated Components for Displacement of Plastic	30
III. Calculated Values of Bone Displacement	34
IV. Calculated Values for Displacement According to Voltage Variation	35
V. Calculated Displacements for Voltage Variations and Corresponding Logarithms	37

C H A P T E R I

INTRODUCTION

Biologically, many systems, if not all, have indicated the presence of piezoelectricity (crystalline material subjected to mechanical stress produces an electric current and conversely, the generation of stress in crystalline material subjected to applied voltage). Different forms of mechanical energy induced in wood, clams, bone, skin, cartilage, arteries, etc... have produced electric potentials of sufficient magnitude to exert a wide range of effects in living systems, including theoretically, control of cell nutrition.¹

Through past research, it is known that bone, a polycrystalline material, is piezoelectric.² In work done by C. A. L. Bassett, '65, deformation of bone, or bending, has shown a positive charge on the convex side and a negative charge on the concave side. Oddly enough, the piezoelectric property holds true even for bone samples that are no longer living. Even bone that has been dried for many years still exhibits this property. It is possible that collagen, apatite, and protein polysaccharides are all involved in the piezoelectric response; however, the precise mechanism for the piezoelectric response in bone is not yet known.

It is strongly believed that electrical stimulation influences growth and the alignment of macromolecules in bone. Stimulation of new bone formation in dog femurs and across rabbit epiphysis by

continuous direct currents has shown a definite polarity effect. The polarity effect has been an increase in bone formation about the cathode and suppression of bone formation at the anode. This implies accumulation of negative charge on concave regions of bone under compression and accumulation of positive charge on convex regions of bone under tension.³ The importance of studying this effect is twofold. First, possibly a better understanding of the electrical response will result. Second, a new and unique method of observation of electrically stressed bone will be available. This method will be compatible with possible clinical application to whole bone.

The nature of work done by other people in bone studies has been extensive and productive in understanding of the piezoelectric response of bone. Four areas of investigation have been the piezoelectric effects in collagen, bone, the biological significance of piezoelectricity, and bone remodeling. The piezoelectric effects in collagen have been observed in materials such as silk, wool, bone, and tendon of ox.⁴ In the study of bone and tendon, work has been centered around characterization and identification of the mechanism involved in the electrical response of bone.⁵

A piezoelectric model for bone remodeling has compared experimental and clinical observations relating to the shape of normal long bones, bone disuse atrophy, the shape of part of long bones during growth, and the growth correction of angular deformity in fractured long bones.⁶ However, most of these investigations were concerned with application of a force or stress to observe the electric polarization. Thus, the mechanism that generates the electrical signal in bone remains unidentified.

Results of studies made in tendon and bone show that the true signal is a square wave voltage in response to a square wave stress; thus, when bone or tendon are stressed, the physiological system produces a corresponding pulse.⁷ In connection with these investigations, hydrostatically applied stress generates voltages that imply the material is pyroelectric (crystals that undergo change in dipole moment when heated). Observations of collagen fibers in tendon of ox and horse through the direct and converse piezoelectric effects has resulted in an estimate of the matrix of piezoelectric constants.⁸

The converse piezoelectric effect in bone (observation of strain resulting from an applied electric field) was observed by Fukada and Yasuda in 1957, but it has received no attention since then in reported work. It seems an effort should be made to observe quantitatively the converse piezoelectric effect. This additional information should provide a more complete picture of the electrical response of bone, which in turn will help in the establishing of a working model for the piezoelectric effect. Thus the purpose of this work is to establish a method for observing effectively the converse piezoelectric response of bone. The experimental technique used is holographic interferometry. It will be demonstrated that the strain in electrically polarized bone can be measured quantitatively and the problems associated with such measurements will be discussed.

Some characteristics of the method (holographic interferometry) used are: it is a non-destructive procedure capable of measuring displacement with magnitude on the order of a wavelength of light of a three dimensional diffusely reflecting object, it is a non-perturbing method whereby the object under investigation need not be handled in

any way, and for small displacement measurements, it is a very sensitive non-contact method allowing the entire surface to be investigated at the same time instead of point-by-point.⁹

C H A P T E R I I

EXPERIMENTAL DESCRIPTION

A. Bone Sample Preparation

In preparing the bone sample, bovine femur, it was necessary to obtain as true a cut as possible according to the following dimensions: .5 cm x 1 cm x 10 cm. Hence, a diamond saw was used to cut the desired parallel beam of bone. After the bone sample was cut, washed with tap water, and soaked in methyl alcohol overnight, a coat of silver conductive paint was painted on the parallel sides of the sample. At the same time, two copper electrodes (no. 32 wire) of twenty centimeter length each were attached to the painted surfaces. Then the sample was mounted rigidly on the specimen table for observation.

The system components for investigation of the bone sample were: a 15 milliwatt helium neon laser, the term deriving its name from the description "light amplification by stimulated emission and radiation," mounting bars (for laser), beam deflector which has two front surface mirrors mounted on a vertical rod allowing the user to direct the beam where needed, a variable beam splitter for varying the beam ratios, three front surface mirrors, two spatial filters which clean the laser beams by eliminating scatter caused by dirt, dust, or minor optical imperfections of components in the system, rotational polaroids for variable attenuators, and a rectangular flat table with

air suspension for vibration isolation. (Note that each of the components was mounted on a magnetic base.) To clarify the arrangement, see Fig. 1 on the next page.

B. Experimental Arrangement

One of the main differences between holography and photography is that the object wave itself is recorded instead of the optically formed image of the object. Once the hologram is developed, the object wave is stored. Illumination of this record will reconstruct the original object wave. However, to clarify holography even more, reference must be made to the object beam and reference beam. The object beam is a monochromatic coherent beam of light which illuminates the object. The reference beam is a beam of monochromatic coherent light that illuminates the film. Both beams are obtained from the same laser beam. Some of the scattered light from the object strikes the film and interferes with the reference beam, since both beams were initially derived from the same coherent source. The result of the interference is a spatial modulation of the optical density of the film. This forms the hologram. Hence, illumination of the hologram with the original reference beam gives a reconstructed wavefront as if it came from the original object without the presence of the object itself. Due to this fact, the biggest advantage of holography is the ability to store enough information about the object in the hologram to produce a true three dimensional image, complete with parallax and depth of focus.¹⁰

In making a hologram, the following must be considered: arranging the components of the system, loading, exposing, and developing the film. The laser beam is kept parallel and at the

Figure 1. The following illustration is for clarification of the basic arrangement used for the proposed experiment. Components involved are: helium neon laser, a vibration isolation table (3' x 4'), 2 spatial filters, one beam splitter, 3 front surface mirrors to direct the beam where desired, specimen table, and hologram plate. Note that the arrangement is such that the beam is 9" from the surface of the vibration isolation table, the optical path lengths are kept equal, and mirror 3 and mirror 1 are placed at positions which allow the laser beam being reflected from their surfaces to be as near parallel as possible.

desired distance from the surface of the table. It is advantageous to maintain optical path lengths equal; however, it is not a necessary condition as long as the difference is less than or equal to the coherence length which is 1.2 meters. Separation distance between hologram plate and object should be small due to the nature of the planned experiment. Position of the object with respect to the photographic film depends on what the observer wants to see. Once the components have been positioned and locked on the vibration isolation table, the intensity measurements of the object and reference beam are taken. A beam ratio (average irradiance at the hologram plane due to the object and the irradiance of the reference beam at the hologram plane) of 6:1 is used. Film loading is done in the dark, once the time of exposure is determined from the overall intensity measurements. Then, the film is exposed for the desired increment of time, sealed tight from light, and developed. Development for Agfa 8E75 high resolution film required 5 minutes in the developer (Kodak D-19), 20 seconds in the stop bath, and 5 minutes in Kodak Rapid Fixer. Then the film was washed with tap water for five more minutes and dried.

Actual holographic arrangements used differed only in two aspects: the separation distance between holographic plate and subject, and the interchange of the reference and object beam directions with respect to the beam splitter. With the first arrangement in mind, i.e., Fig. 1 from preceding page, the beam of bone was supported rigidly on a specimen table at one end, while the opposite end was free to move. The distance between the film plate and specimen was 5.4 centimeters, the specimen was oriented normal to the film plate, and the particular spot of observation on the bone surface was at

22.7 centimeters from the rectangular flat table.

C. Holographic Analysis

Since information on the displacement of bone due to an applied electric field is sought, double-exposed holograms are used for such observations. A double-exposed hologram records a permanent record of the change in object between exposures due to various factors such as strain, stress, electric fields, thermal change, air resistance, and moisture content. Changes in the optical paths give rise to interference patterns which are seen whenever the hologram is viewed by the observer with a reconstructed wave identical to the original reference wave. Fringes are dependent upon subject deformation. Therefore, observation of these fringe patterns along with the mathematical manipulations will determine the displacement in bone caused by an applied electric field.¹¹

The approach used for interpretation of the doubly-exposed holograms is that developed by Aleksandrov and Bonch-Bruevich.¹² Geometrically, the surface being displaced can be represented as shown in Fig. 2. Figure 2 illustrates a relation between displacement and associated fringe patterns. A diffusely reflecting surface, ABC, is displaced to the position A'B'C'. Since pure translation is being illustrated, segments AA', BB', and CC' have the equivalent displacement vector $\vec{\Delta r}$. The observer considers the interference of light from the corresponding points such as A and A' and relates this to the displacement vector $\vec{\Delta r}$.¹³

Illumination of the diffusely reflecting surface is in the direction of the unit vector \vec{n}_i . Observation of the scattering light rays is in the direction of the unit vector \vec{n}_s , where \vec{n}_i and \vec{n}_s are in

Figure 2. The following illustration shows a surface ABC and its corresponding translation A'B'C'. Since double exposure interferometry is used in the experiment, the illustration of surface ABC corresponds to the first exposure of the hologram and surface A'B'C' corresponds to the second exposure of the hologram. Note that for each incident angle, there is a corresponding scattering angle from surfaces ABC and A'B'C'. The line segment connecting points A and A' is the vector displacement, $\Delta\vec{r}$, that is sought in the experiment resulting from an electrically induced strain.

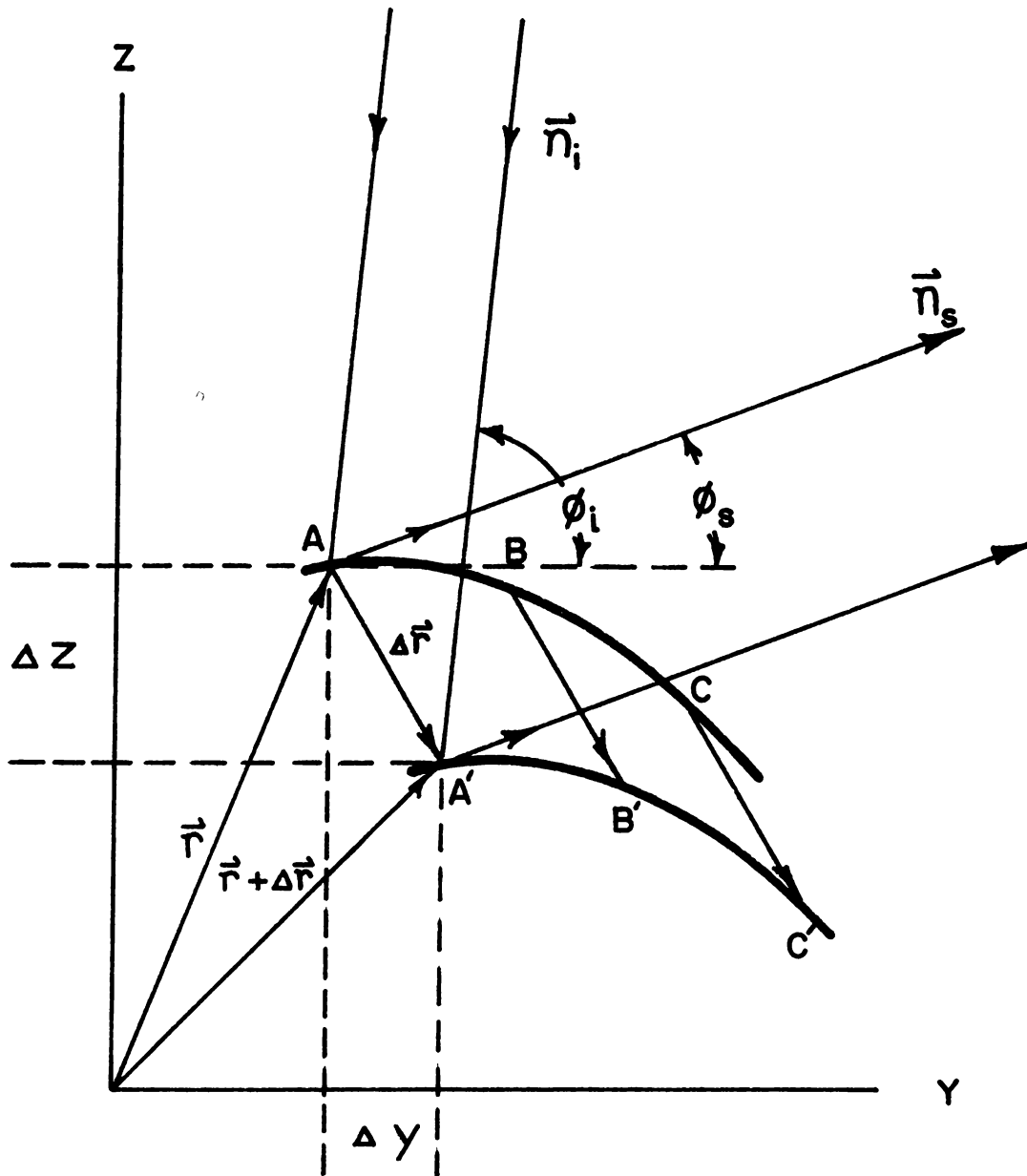


Figure 2. Pure translation of a surface.

the yz plane. The direction of propagation is important in determining the difference in phase, δ , of light traveling from source to observer. There are two distinct optical paths, illuminating and scattering. The change in phase of the illuminating beam due to the surface displacement, $\Delta\vec{r}_i$, is $(2\pi/\lambda)\Delta\vec{r}_i \cdot \vec{n}_i$ and the change in phase for the scattered beam due to surface displacement is $(2\pi/\lambda)\Delta\vec{r}_i \cdot \vec{n}_s$. Hence, a general statement of the phase difference is:

$$(1) \quad \delta = \left(\frac{2\pi}{\lambda}\right) \left[\Delta\vec{r} \cdot (\vec{n}_s - \vec{n}_i) \right] .$$

To relate fringe observation to surface displacement, the subject is focused through a small aperture, such as the iris of the eye. The observer considers the interference of light rays scattered from pairs of corresponding points on the original and deformed surfaces. Fringe patterns may develop on the surface, near the surface, or at a great distance from the surface (distance here being in terms of wavelength of light). The increased depth of field resulting from the small aperture allows the surface and fringes to be in focus simultaneously. Once the original and deformed surface as well as the fringe patterns are in focus, a series of observations are made to determine the displacement of a small area on the surface. For a particular direction of observation, \vec{n}_{s_o} , the phase difference, δ_o , between rays scattered from the spot in its displaced and original positions is:

$$(2) \quad \delta_o = \frac{2\pi}{\lambda} \left[\Delta\vec{r} \cdot (\vec{n}_{s_o} - \vec{n}_i) \right] .$$

Next, the spot is sighted from a new viewing position \vec{n}_{s_k} , remembering to count the number of fringes that pass the spot in question. The phase difference for this direction of observation corresponding to

\vec{n}_{s_k} is:

$$(3) \quad \delta_k = \frac{2\pi}{\lambda} \left[\Delta\vec{r} \cdot (\vec{n}_{s_k} - \vec{n}_i) \right] .$$

Hence, the difference is:

$$(4) \quad \delta_k - \delta_o = \frac{2\pi}{\lambda} \left[\Delta\vec{r} \cdot (\vec{n}_{s_k} - \vec{n}_i - \vec{n}_{s_o} + \vec{n}_i) \right] .$$

The passage of one complete fringe corresponds to a change of phase of 2π ; thus, rewriting eq. (4) in terms of the number of fringes that pass the observed point, we have:

$$(5) \quad \frac{2\pi}{\lambda} \left[\Delta\vec{r} \cdot (\vec{n}_{s_k} - \vec{n}_{s_o}) \right] = \pm 2\pi K ,$$

where $2\pi K$ is the number of radians corresponding to the passage of K fringes through the spot in question and the \pm sign indicates the direction of fringe movement (left or right of point of observation). Thus eq. (5) becomes

$$(6) \quad \Delta\vec{r} \cdot \Delta\vec{n} = \pm K\lambda ,$$

where $\Delta\vec{n}$ represents the difference in the unit vector \vec{n}_{s_k} and \vec{n}_{s_o} . Equation (6) represents a linear system of equations in three unknowns, the three components of $\Delta\vec{r}$. The change in direction of each observation is only possible within limits of the "window" through which the object is viewed; i.e., through the hologram.¹⁴ In order for the observations of the fringe shifts to yield the best estimate of the surface displacement, the method of least squares is used. In this method, four separate sets of observations are used yielding four equations with three unknowns. Hence, the use of matrices is to represent four sets of observations in matrix form. The observations

will be a $\vec{\Psi}_i$ vector (components of $\vec{\Psi}_i$ are the $\pm K\lambda$) for $i = 1, 2, 3, \dots, n$; hence,

$$\vec{\Psi} = \begin{pmatrix} \Psi_1 \\ \Psi_2 \\ \Psi_3 \\ \vdots \\ \Psi_n \end{pmatrix}$$

and X will be the matrix of n observations on x_{ij} , y_{ij} , and z_{ij} variables, for $i = 1, 2, 3, \dots, n$ and $j = 1, 2, 3$; therefore,

$$X = \begin{pmatrix} x_{11} & y_{12} & z_{13} \\ x_{21} & y_{22} & z_{23} \\ x_{31} & y_{32} & z_{33} \\ \vdots & \vdots & \vdots \\ x_{n1} & y_{n2} & z_{n3} \end{pmatrix},$$

where the x, y, and z's are the components of $\Delta\vec{n}$. If \vec{e} is the vector of components e_i , $i = 1, 2, 3, \dots, n$, that represent the deviation of the observed $\vec{\Psi}_i$ from their expected values, then we have the following:

$$(7) \quad \vec{\Psi}_i = r_1 x_{i1} + r_2 y_{i2} + r_3 z_{i3} + e_i,$$

for $i = 1, 2, 3, \dots, n$. Having defined the X matrix and the two vectors $\vec{\Psi}$ and \vec{e} as above, the following statement can now be made:

$$(8) \quad \vec{\Psi} = X\vec{r} + \vec{e},$$

where \vec{r} is the displacement vector to be estimated;

$$\vec{r} = \begin{pmatrix} r_1 \\ r_2 \\ r_3 \end{pmatrix}.$$

Thus the method of least squares involves minimizing the sum of the squares of the elements of the vector \vec{e} in eq. (8). (Note that minimizing the square of deviation with respect to r yields eq. (8); see reference 15.) The fortran program listed in Appendix I makes use of eq. (8) to give a computed value for the components of the vector displacement.

C H A P T E R I I I

EXPERIMENTAL DISCUSSION

A. Electrical Response of Bone

Since the theoretical aspect for mathematical computation has been presented, the experimental data is now centered around a piece of plastic material that has been displaced by the rotation of the barrel of a micrometer fixed rigidly on a specimen table. Obtaining a direct reading with the micrometer of the plastic's movement and computing the same movement with the given mathematics gives a check on the prescribed procedure.

Development of three basic holograms is the source of information for bending in the bone. Each hologram considered varied only in the particular surface being observed. Because the bone was cut purposely in rectangular shape, the variation of bone surface hologrammed was due to consecutive 90° rotations.

Hence, the following are computations of displacement of the plastic material and of the sides of the bone; however, the inner surface (surface adjacent to bone marrow) was not hologrammed. Once all the components are evaluated and a value for $\Delta \vec{r}$ is computed, then the information is written in succeeding tables, depending on the surface of observation.

Although experimental error does exist, the direct measurement of the movement of the plastic was the actual rotation of the

Figure 3. The following illustration points out a sequence of four observations in the plane of the hologram plate. Each observation, from $P_1 \rightarrow P_2$, passes through the origin, 0, and the length of the line segment $\bar{P}_1\bar{P}_2$ depends on the dimensions of the film inside the hologram plate.

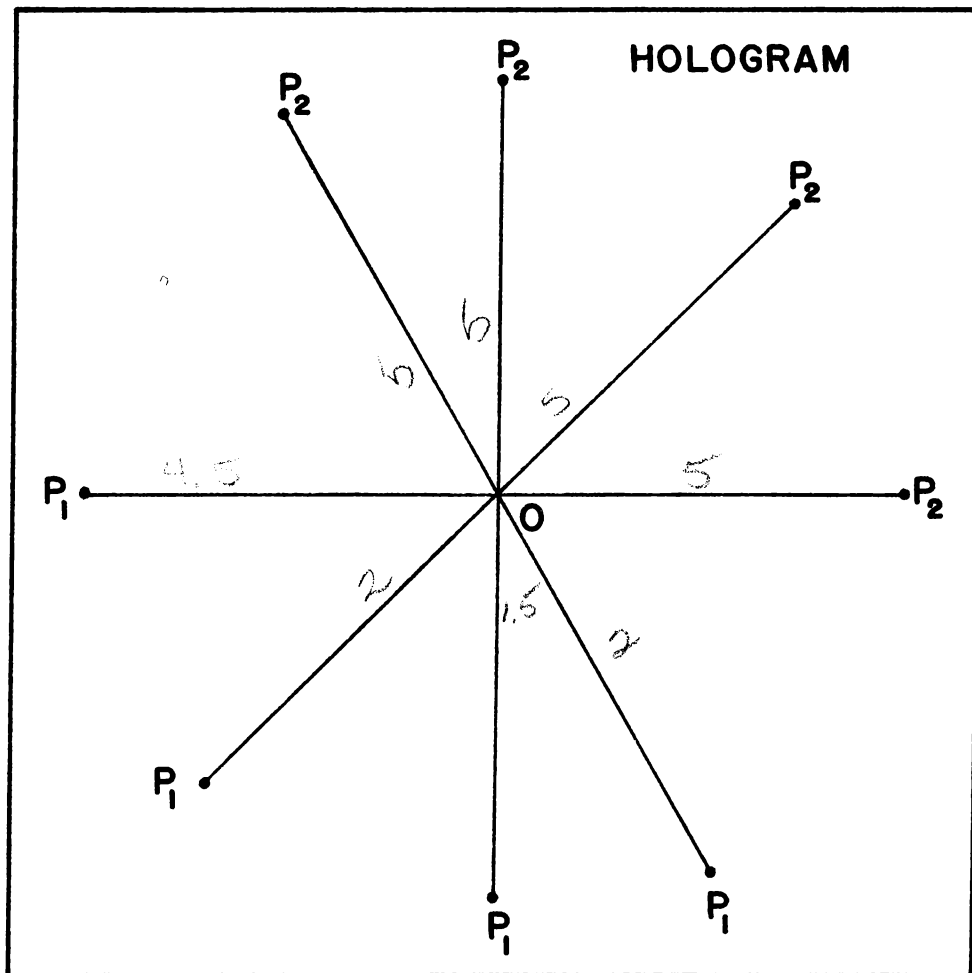


Figure 3. Points of observation where observer is normal to hologram plate.

Figure 4. The origin O' is located at the point of interest on the image of the particular surface. The origin O is located in the plane of the hologram by the intersection x' with that plane. The point O' is observed from the direction $O'P_1$ to $O'P_2$ with the number of fringe shifts counted while going from the direction $O'P_1$ to $O'P_2$. The unit vectors n_1 and n_2 are to be resolved into their components along the x , y , and z directions in terms of the angles θ_1 , θ_2 , α_1 , and α_2 .

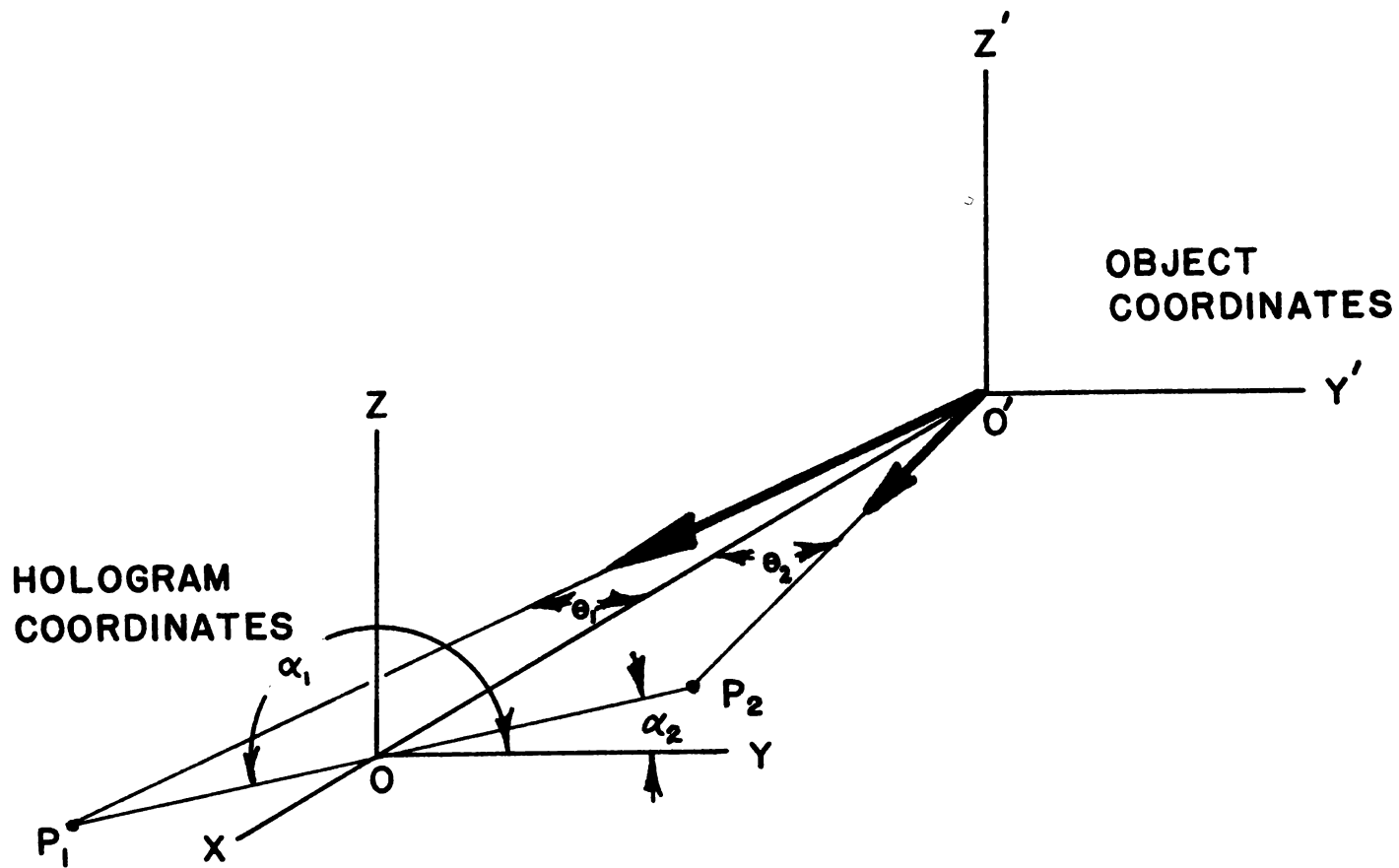


Figure 4. Geometrical lay-out for observations

barrel of a micrometer with an accuracy of .0001 of an inch. Calculation of the movement with a system of four equations gave a computed value of displacement within 5% of the measured value. Thus, the same procedure was followed using the bone. The only deviation from the procedure was the application of an electric field for deformation of the bone surface in question.

Surface: Plastic material.

Ratio of reference to object beam: 1:1.

Optical path lengths: 126 centimeters.

Beam splitter was set on no. 5 and one variable attenuator was used on reference beam.

Table I. Data for calculated displacement of plastic. The four observations, $P_1 \rightarrow P_2$, are listed with the corresponding direction and number of fringes passing the particular point of observation on the object's surface.

Table I
Data for Calculated
Displacement of Plastic

Direction of Fringe Movement	Observation $P_1 \rightarrow P_2$	Number of Fringes
P_2 to P_1	horizontal	4
P_2 to P_1	45° angle	5
P_2 to P_1	vertical	3
P_2 to P_1	60° angle	3

For the horizontal observation:

$$\begin{aligned}n_{1x} &= n \cos \theta_1 \\ &= \frac{5.4 \text{ cm}}{5.7 \text{ cm}} \\ &= 0.947,\end{aligned}$$

$$\begin{aligned}n_{1y} &= n \sin \theta_1 \\ &= -\frac{2 \text{ cm}}{5.7 \text{ cm}} \\ &= -0.350,\end{aligned}$$

and $n_{1z} = \text{zero}$.

$$\begin{aligned}n_{2x} &= n \cos \theta_2 \\ &= \frac{5.4 \text{ cm}}{5.9 \text{ cm}} \\ &= 0.915,\end{aligned}$$

$$\begin{aligned}n_{2y} &= n \sin \theta_2 \\ &= \frac{2.5 \text{ cm}}{5.9 \text{ cm}} \\ &= 0.423,\end{aligned}$$

and $n_{2z} = \text{zero}$.

For the 45° angle observation:

$$\begin{aligned} n_{1x} &= n \cos \theta_1 \\ &= \frac{5.40 \text{ cm}}{5.49 \text{ cm}} \\ &= 0.983, \end{aligned}$$

$$\begin{aligned} n_{1y} &= n \sin \theta_1 \cos \alpha_1 \\ &= \left(\frac{1 \text{ cm}}{5.49 \text{ cm}} \right) (-.707) \\ &= -0.128, \end{aligned}$$

$$\begin{aligned} \text{and } n_{1z} &= n \sin \theta_1 \sin \alpha_1 \\ &= \left(\frac{1 \text{ cm}}{5.49 \text{ cm}} \right) (-.707) \\ &= -0.128. \end{aligned}$$

$$\begin{aligned} n_{2x} &= n \cos \theta_2 \\ &= \frac{5.4 \text{ cm}}{6.1 \text{ cm}} \\ &= 0.885, \end{aligned}$$

$$\begin{aligned} n_{2y} &= n \sin \theta_2 \cos \alpha_2 \\ &= \left(\frac{3 \text{ cm}}{6.1 \text{ cm}} \right) (.707) \\ &= 0.347, \end{aligned}$$

$$\begin{aligned} \text{and } n_{2z} &= n \sin \theta_2 \sin \alpha_2 \\ &= \left(\frac{3 \text{ cm}}{6.1 \text{ cm}} \right) (.707) \\ &= 0.347. \end{aligned}$$

For the vertical observation:

$$\begin{aligned}n_{1x} &= n \cos \theta_1 \\ &= \frac{5.40 \text{ cm}}{5.49 \text{ cm}} \\ &= 0.983,\end{aligned}$$

$$n_{1y} = \text{zero},$$

$$\begin{aligned}\text{and } n_{1z} &= n \sin \theta_1 \\ &= -\frac{1 \text{ cm}}{5.49 \text{ cm}} \\ &= -0.182.\end{aligned}$$

$$\begin{aligned}n_{2x} &= n \cos \theta_2 \\ &= \frac{5.40 \text{ cm}}{5.90 \text{ cm}} \\ &= 0.915,\end{aligned}$$

$$n_{2y} = \text{zero},$$

$$\begin{aligned}\text{and } n_{2z} &= n \sin \theta_2 \\ &= \frac{2.5 \text{ cm}}{5.9 \text{ cm}} \\ &= 0.423.\end{aligned}$$

For the 60° angle observation:

$$\begin{aligned} n_{1x} &= n \cos \theta_1 \\ &= \frac{5.40 \text{ cm}}{5.49 \text{ cm}} \\ &= 0.983, \end{aligned}$$

$$\begin{aligned} n_{1y} &= n \sin \theta_1 \cos \alpha_1 \\ &= \left(\frac{1 \text{ cm}}{5.49 \text{ cm}} \right) (.500) \\ &= 0.091, \end{aligned}$$

$$\begin{aligned} \text{and } n_{1z} &= n \sin \theta_1 \sin \alpha_1 \\ &= \left(\frac{1 \text{ cm}}{5.49 \text{ cm}} \right) (-.866) \\ &= -0.157. \end{aligned}$$

$$\begin{aligned} n_{2x} &= n \cos \theta_2 \\ &= \frac{5.4 \text{ cm}}{6.1 \text{ cm}} \\ &= 0.885, \end{aligned}$$

$$\begin{aligned} n_{2y} &= n \sin \theta_2 \cos \alpha_2 \\ &= \left(\frac{3 \text{ cm}}{6.1 \text{ cm}} \right) (-.500) \\ &= -0.245, \end{aligned}$$

$$\begin{aligned} \text{and } n_{2z} &= n \sin \theta_2 \sin \alpha_2 \\ &= \left(\frac{3 \text{ cm}}{6.1 \text{ cm}} \right) (.866) \\ &= 0.425. \end{aligned}$$

Hence, the components of the vector displacement, $\Delta \vec{r}$, are evaluated.

Table II. Calculated components for displacement of plastic. Listings in the table give the corresponding values of the components, x , y , and z , for each observation. The values of $K\lambda$ are the result of the product of the number of fringes passing the point in question and the wavelength of the laser (632.8 nm).

Table II
 Calculated Components
 for
 Displacement of Plastic

	$K\lambda$ (cm)	x	y	z
horizontal	-2.53×10^{-4}	-.032	.773	0
45° angle	-3.16×10^{-4}	-.098	.475	.475
vertical	-1.89×10^{-4}	-.068	0	.605
60° angle	-1.89×10^{-4}	-.098	-.336	.582

Computed value of displacement in plastic: 16.16×10^{-4} cm.

Figure 5. The following figure is a photograph of an illuminated hologram. The image in the hologram is a horizontal beam of bone with an applied electric field of 400 volts. Dark lines on the bone surface are the fringe pattern resulting from the electrically induced strain. Note, the movement of these dark bands is used for calculating the vector displacement, $\Delta\vec{r}$, of a point on the surface.

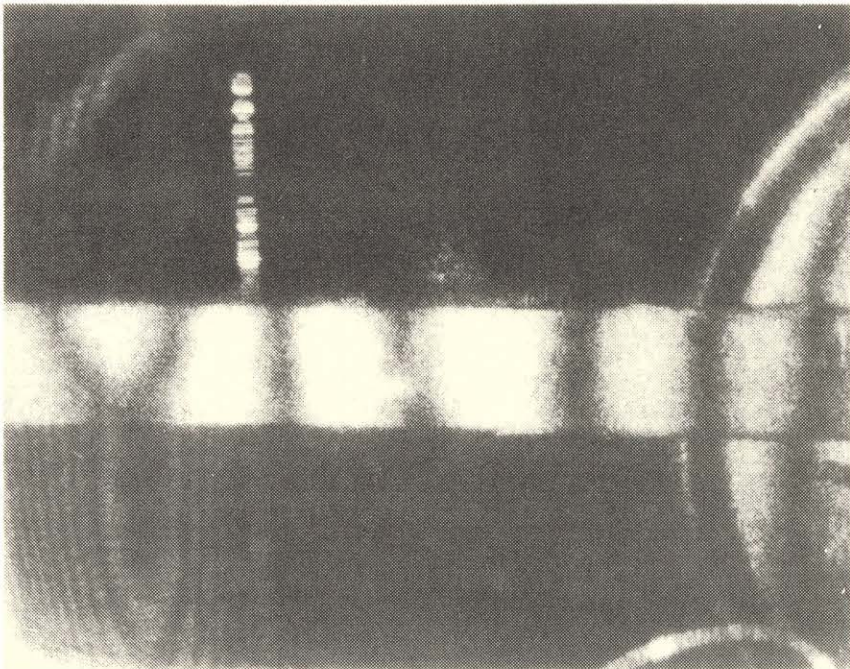


Figure 5. Photograph of an illuminated hologram.

Table III. Calculated values of bone displacement. Listings in the table are the corresponding components, x, y, and z, for each observation of three different sides of the beam of bone. Note, for each bone surface, there is a computed displacement, $\Delta\vec{r}$.

Table III

Calculated Values of Bone Displacement

Bone Surface 1 ($\lambda = 632.8$ nm)

$\pm K$	$K\lambda$ (cm)	x	y	z
6	3.796×10^{-4}	-0.079	0.758	0
0.5	0.316×10^{-4}	-0.178	0.550	0.550
-5	-3.164×10^{-4}	-0.098	0	0.673
-7	-4.429×10^{-4}	-0.098	-0.336	0.582

Computed $\Delta \vec{r} = 7.04$ microns.

Bone Surface 2

-8	-5.062×10^{-4}	-0.062	0.841	0
-5	-3.164×10^{-4}	-0.098	0.475	0.475
-2	-1.265×10^{-4}	-0.036	0	0.532
-3	-1.898×10^{-4}	-0.098	-0.336	0.582

Computed $\Delta \vec{r} = 20.08$ microns.

Bone Surface 3

7	4.429×10^{-4}	-0.077	0.746	0
2	1.265×10^{-4}	-0.096	0.468	0.468
-6	-3.796×10^{-4}	-0.035	0	0.522
-7	-4.429×10^{-4}	0.073	-0.295	0.512

Computed $\Delta \vec{r} = 8.80$ microns.

Table IV
 Calculated Values for Displacement
 According to Voltage Variation*

Observation $P_1 \rightarrow P_2$	$\pm K\lambda$ (cm)	x	y	z	Voltage
I. horizontal	3.796×10^{-4}	-0.079	0.758	0	400
45° angle	0.316×10^{-4}	-0.178	0.550	0.550	
vertical	-3.164×10^{-4}	-0.098	0	0.673	
60° angle	-4.429×10^{-4}	-0.098	-0.336	0.582	
Computed $\Delta \vec{r} = 7.04$ microns.					
II. horizontal	-1.265×10^{-4}	-0.097	0.674	0	600
45° angle	-2.531×10^{-4}	-0.021	0.381	0.381	
vertical	-3.796×10^{-4}	-0.004	0	0.454	
60° angle	-3.164×10^{-4}	-0.004	-0.227	0.394	
Computed $\Delta \vec{r} = 16.64$ microns.					
III. horizontal	-1.582×10^{-4}	Note: x,y,z components			800
45° angle	-1.898×10^{-4}	same as preceding			
vertical	-3.164×10^{-4}	set.			
60° angle	-2.214×10^{-4}				
Computed $\Delta \vec{r} = 24.16$ microns.					

*Note, the x, y, and z components of II, III, and IV are identical, but the computed displacement, $\Delta \vec{r}$, increases due to the application of a greater electrical strain.

Table IV, continued

IV.	horizontal	-4.429×10^{-4}				x,y,z components	1100
	45° angle	-1.898×10^{-4}				same as preceding	
	vertical	-1.898×10^{-4}				set.	
	60° angle	-2.531×10^{-4}					
	Computed $\Delta \vec{r} = 65.15$ microns.						
V.	horizontal	-1.582×10^{-4}	-0.008	0.228	0		1400
	45° angle	0.316×10^{-4}	-0.019	0.213	0.213		
	vertical	1.582×10^{-4}	-0.019	0	0.301		
	60° angle	1.582×10^{-4}	-0.008	-0.114	0.197		
	Computed $\Delta \vec{r} = 290.11$ microns.						
VI.	horizontal	-3.164×10^{-4}	-0.013	0.295	0		2000
	45° angle	-5.062×10^{-4}	-0.034	0.273	0.273		
	vertical	-4.429×10^{-4}	-0.034	0	0.387		
	60° angle	-3.796×10^{-4}	-0.013	-0.147	0.256		
	Computed $\Delta \vec{r} = 499.44$ microns.						

Table V
 Calculated Displacements for Voltage Variations
 and
 Corresponding Logarithms*

Displacement	Log of Displacement	Voltage	Log of Voltage
7×10^{-4} cm	.084	400	2.602
16×10^{-4} cm	1.204	600	2.778
24×10^{-4} cm	1.380	800	2.903
65×10^{-4} cm	1.812	1100	3.041
290×10^{-4} cm	2.462	1400	3.146
499×10^{-4} cm	2.698	2000	3.301

*Listings in the table for displacements at varied voltages are taken from Table IV.

Figure 6. Plot of logarithms of the displacement versus the magnitude of the applied voltage. The straight line is at least square fit to the data of Table V and has a slope of 3.9.

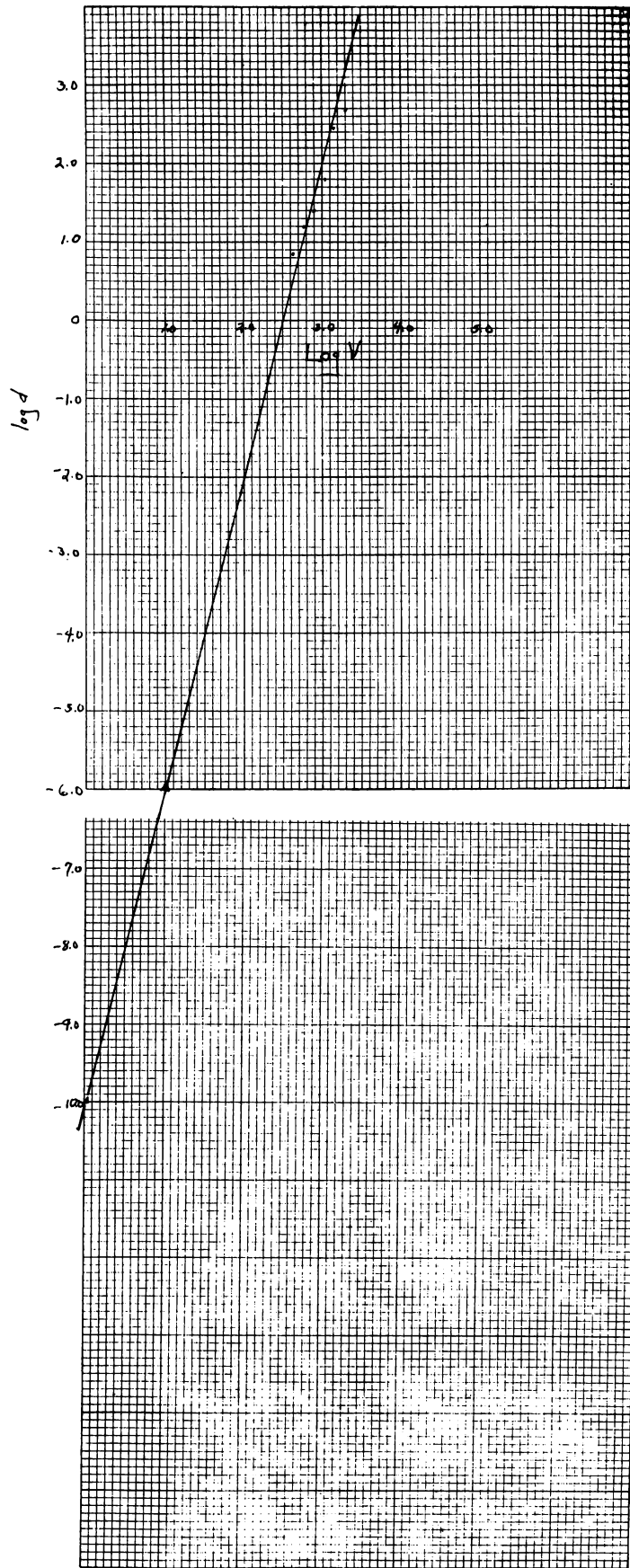


Figure 6. Plot of logarithms of the displacement versus the magnitude of the applied voltage.

One direct application using the technique established in this work is to measure the dependence of displacement on applied voltage. The range of voltage was from 400 to 2000 volts, each time computing a corresponding displacement. The data is plotted on a log-log scale yielding a straight line.^{15,16,17} A least squares fit to the data yields a line of slope 3.9. Thus, the relation between displacement and voltage is

$$(9) \quad d = a V^b ,$$

where a , the y-intercept, is -10 , and b , the slope, is 3.9 . Note, in the above equation,

$$a = \frac{\sum_{i=1}^M d_i \sum_{i=1}^M V_i^2 - \sum_{i=1}^M V_i d_i \sum_{i=1}^M V_i}{\sum_{i=1}^M V_i^2 - \frac{(\sum_{i=1}^M V_i)^2}{M}}$$

and

$$b = \frac{m \sum_{i=1}^M V_i d_i - \sum_{i=1}^M d_i \sum_{i=1}^M V_i}{m \sum_{i=1}^M V_i^2 - \frac{(\sum_{i=1}^M V_i)^2}{M}}$$

where m is the number of measurements and M is any positive integer.

C H A P T E R I V

CONCLUSION

The purpose of this work was to establish the techniques of holographic interferometry as applied to the study of the piezoelectric response of bone. To this end, the holographic procedures and methods of analysis have been accomplished.

The double exposure holographic interferogram has been applied to the observation of small displacements of bone that has been electrically stressed. As a check, the same procedure was applied to the known displacement of a piece of plastic material being displaced with a micrometer. The agreement between known displacement and calculated value for the plastic material was within 5%.

As an application of the holographic techniques as applied to the electrical response of bone, the displacement was measured as a function of applied potential. The measurements yield a $V^{3.9}$ power dependence of the displacement on the potential. This information should prove useful to others interested in the electrical response of bone.

The establishment of this technique as applied to bone lays the ground work for additional work in the study of how bone responds to electrical stimulation. Two direct applications will be the examination of the dependence of the displacement amplitudes on the frequency of the applied potential and the mapping of the displacement over whole bone surfaces due to different electrode arrangements.

A P P E N D I X I

Programmed Solution for a Set

of

Linearly Independent Nonhomogeneous Equations

```
DIMENSION A(11,11),B(11,20),C(20,20),D(11,11)
```

```
DIMENSION E(11,11),F(11)
```

```
LAL=11
```

```
LBL=11
```

```
MBL=20
```

```
ICK=0
```

C.....READING IN THE VALUES OF THE SIDES OF THE MATRIX AND THE LETTER

C.....SO YOU CAN TELL WHICH SUBROUTINE TO GO TO.

```
READ(8,2) LA, LB, MB, IDEC
```

```
2   FORMAT(3I10, 49X, A1)
```

C.....READING IN THE MATRIX.

```
READ(8,5) ((B(I,J), J=1, 10), I=1, LB)
```

```
5.....FORMAT(5E16.6/5E16.6)
```

C.....WRITING OUT THE INPUT MATRIX.

```
WRITE(5,203)
```

```
203  FORMAT(1H1, 10X, THE INPUT MATRIX IS ,//)
```

```
DO 201 NF=1,LA
```

```
WRITE(5,200) (B(NF,NG), NG=1, MB)
```

```
200  FORMAT(1X,10E13.6)
```

```
201  WRITE(5,202)
```

```
202  FORMAT(/// )
```

```
LBJ=MB+1
```

C.....DECIDING WHICH SUBROUTINE TO GO TO.

```
IF(1HI. EQ. IDEC) GO TO 1000
```

```
IF(MB. NE. 10) GO TO 75
```

C.....IF YOUR MATRIX IS A TEN BY TEN, THEN READ IN THE CONSTANTS

C.....OF THE EQUATIONS

```
      READ(8,5) (B(MO,11), MO=1, LB)
C.....GO TO SUBROUTINE EQU.
75   WRITE(5,204)
204  FORMAT(1H1, 42X, THE CONSTANTS TO THE EQUATIONS IN THE MATRIX ARE)
      WRITE(5,205) (B(NH,LBJ), NH=1, LB)
205  FORMAT(53X, E16.6, ///)
      IF(LB .EQ. MB) GO TO 400
      CALL NSQ(A,B,C,LA,LB,MB,LAL,LBL,MBL,D,E,F)
      GO TO 10001
400  CALL EQU(A,B,C,LA,LB,MB,LAL,LBL,MBL,      )
      GO TO 10001
C.....MAKE THE WIDTH TWICE AS WIDE BECAUSE YOU ARE ABOUT TO USE
C.....SUBROUTINE INV.
10000 MB=MB*2
C.....GO TO SUBROUTINE INV.
      CALL INV(A,B,C,LA,LB,MB,LAL,LBL,MBL,D      )
10001 CALL EXIT
      END
```

```

SUBROUTINE INV(A,B,C,LA,LB,MB,LAL,LBL,MBL,D
)
DIMENSION A(LAL,LBL),B(LBL,MBL),C(LAL,MBL),D(LAL,LBL)

LBJ=LB+1

MH=MB/2

C.....PUTTING MATRIX B INTO MATRIX D.

DO 12o MF=1, LB
DO 12o MG=1, MH
12o D(MF,MG)=B(MF,MG)

C.....GO TO SUBROUTINE ZERO.

CALL ZERO(A,LB,LA,LB,MB,LAL,LBL,MBL)

C.....PUT MATRIX A IN MATRIX B. PUT IT IN THE LOCATIONS TO THE RIGHT
C.....OF WHAT IS ALREADY IN MATRIX B.

DO 52 I=1, LB
K=o
DO 52 J=LBJ, MB
K=K+1
52 B(I,J) = A(I,K)
DO 54 JA=1, LB

C.....FINDING THE TRANSFORMATION MATRIX FOR EACH COLUMN.

IF(I .EQ. JA) GO TO 53
DO 53 I=1, LA
A(I,JA)=- (B(I,JA)/B(JA,JA))
53 CONTINUE

CALL MULT(A,B,C,LA,MB,LB,LAL,LBL,MBL)

C.....PUT MATRIX A INTO MATRIX B.

59 DO 57 IC=1, LA
DO 57 JC=1, MB

```

```

57   B(IC,JC)=C(IC,JC)
C.....GO TO SUBROUTINE ZERO.
      CALL ZERO(A,LB,LA,LB,MB,LAL,LBL,MBL)
54   CONTINUE
C.....GO TO SUBROUTINE ZERO.
      CALL ZERO(A,LB,LA,LB,MB,LAL,LBL,MBL)
58   DO 60 IA=1,LB
60   A(IA,IA)=(1/B(IA,IA))
C.....GO TO SUBROUTINE MULT.
      CALL MULT(A,B,C,LA,MB,LB,LAL,LBL,MBL)
      MA=0
C.....CHECKING IF ONE OF THE NUMBERS IN THE DIAGONAL OF A IS ZERO
C.....AFTER MULTIPLICATION.
      DO 81 KE=LBJ,MB
      MA=MA+1
      IF(C(MA,KE) .NE. 0.) GO TO 81
C.....IF ONE OF THE NUMBERS IN THE DIAGONAL IN B IS ZERO, THEN WRITE
C.....OUT AN ERROR MESSAGE.
      WRITE(5,83)
83   FORMAT(5X, SORRY CHARLEY, YOU CAN NOT FIND THE MATRIX INVERSION
      1, BY THE GAUSS REDUCTION TECHNIQUE)
      GO TO 82
81   CONTINUE
C.....WRITING OUT THE INVERTED MATRIX.
      WRITE(5,102) LB
102  FORMAT(1H1,10X, THE MATRIX INVERSION BY THE GAUSS REDUCTION
      TECHNIQUE IS BELOW , I4, ROWS AND COLUMNS ,      //)

```

```
DO 79 LC=1,LA
WRITE(5,78) (C(LC,LD), LD=LBJ,MB)
78  FORMAT(1X,10E13.6)
79  WRITE(5,140)
140  FORMAT(///      )
DO 141 NE=1,LB
ND=0
DO 141 NC=LBJ,MB
ND=ND+1
141  B(NE,ND)=C(NE,NC)
CALL MULT(D,B,C,LA,MH,LB,LAL,LBL,MBL  )
WRITE(5,121)
121  FORMAT(1H1,10X,  WHEN ONE MULTIPLIES B AND B INVERSE TOGETHER
1, THE RESULTS ARE , //  )
DO 122 LC=1,LA
WRITE(5,78) (C(LC,LD), LD=1, MH)
122  WRITE(5,140)
82  RETURN
END
```

```
SUBROUTINE EQU(A,B,C,LA,LB,MB,LAL,LBL,MBL)
DIMENSION A(LAL,LBL), B(LBL,MBL), C(LAL,MBL)
LBJ=LB+1
AV=0
IB=MB+1
C.....MAXIMIZING THE MATRIX.
DO 10 JD=1, MB
IF=0
DO 11 II=JD, LB
IF(B(JD,JD) .GE. B(II,JD)) GO TO 11
IF=II
11 CONTINUE
IF(IF .EQ. 0) GO TO 1090
DO 14 IS=1,IB
EXCH=B(JD,IS)
B(IF,IS)=B(IF,IS)
14 B(IF,IS)=EXCH
C.....GO TO SUBROUTINE ZERO.
1090 DO 50 IO=1,LB
DO 50 JO=1,LB
IF(IO .EQ. JO) GO TO 51
A(IO,JO)=0.
GO TO 50
51 A(IO,JO)=1.
50 CONTINUE
C.....CHECKING IF THERE IS A ZERO IN THE DIAGONAL.
IF(ABS(B(JD,JD)) .GT. .00001) GO TO 90
```

```
IF(ABS(B(JD,IB)) .GT. .00001) GO TO 91
GO TO 92
C.....FINDING THE TRANSFORMATION MATRIX FOR EACH COLUMN.
90 DO 70 IG=1,LB
IF(JD .EQ. IG) GO TO 70
A(IG,JD)=- (B(IG,JD)/B(JD,JD))
70 CONTINUE
C.....GO TO SUBROUTINE MULT.
CALL MULT(A,B,C,LA,IB,LB,LAL,LBL,MBL )
C.....PUTTING THE RESULTS OF SUBROUTINE MULT C, INTO MATRIX B.
DO 77 KA=1,LA
DO 77 KB=1,IB
77 B(KA,KB)=C(KA,KB)
10 CONTINUE
GO TO 108
C.....TELLING THE PROGRAMMER THAT THERE ARE NO SOLUTIONS FOR THIS
C.....MATRIX
91 WRITE(5,103)
103 FORMAT(7X, THERE ARE NO SOLUTIONS FOR THIS MATRIX )
GO TO 109
C.....TELLING THE PROGRAMMER THAT THERE ARE AN INFINITE NUMBER OF
C.....SOLUTIONS.
92 WRITE(5,104)
104 FORMAT(8X, THERE ARE AN INFINITE NUMBER OF SOLUTIONS FOR THIS
1 MATRIX )
GO TO 109
108 DO 105 MC=1,LB
```

```
105  A(1,MC)=B(MC,IB)/B(MC,MC)
      WRITE(5,111)
111  FORMAT(1H1,42X,  THE SOLUTIONS TO THE SYSTEMS OF EQUATIONS ARE  )
C.....WRITING OUT THE SOLUTIONS TO THE SYSTEM OF EQUATIONS.
200  DO 107 MD=1,LB
107  WRITE(5,106) MD, A(1,MD)
106  FORMAT(58X, 1HY, I2, 1H=.E16.6      )
109  RETURN
      END
```

```
      SUBROUTINE MULT(A,B,C,LA,MB,LB,LAL,LBL,MBL      )
C.....THIS SUBROUTINE MULTIPLIES THE TWO MATRICES, A AND B.
      DIMENSION A(LAL,LBL), B(LBL,MBL), C(LAL,MBL)
      DO 1 J=1,LB
C.....THIS LINE ZEROES OUT THIS PRESENT LOCATION.
      C(K,J)=0.
      DO 1 I=1,LB
1      C(K,J)=C(K,J) + A(K,I) * B(I,J)
      RETURN
      END
```

```
      SUBROUTINE ZERO(A, LB, LA, LB, MB, LAL, LBL, MBL )
      DIMENSION A(LAL, LBL)
      C.....THIS SUBROUTINE PUTS THE MATRIX A   1 0 0
      C.....IN THE ARRANGEMENT THAT IS SHOWN   0 1 0
      C.....ON THE SIDE OF THESE COMMENTS.     0 0 1
55     DO 50 IO=1, LB
          DO 50 JO=1, LB
              IF(IO .EQ. JO) GO TO 51
              A(IO, JO)=0.
              GO TO 50
51     A(IO, JO)=1.
50     CONTINUE
      RETURN
      END
```

```

SUBROUTINE NSQ(A,B,C,LA,LB,MB,LAL,LBL,MBL,D,E,F  )
DIMENSION A(LAL,LBL), B(LBL,MBL), C(LAL,MBL), D(LAL,LBL)
DIMENSION E(LAL,LBL), F(LAL)
AV=0.
DO 950 JR=1,LB
950  F(JR)=B(JR,MB+1)
DO 902 IQ=1,MB
DO 902 IR=1,LB
902  E(IQ,IR)=B(IR,IQ)
CALL MULT(E,B,C,LA,MB,LB,LAL,LBL,MBL  )
DO 951 JS=1,MB
DO 951 JT=1,MB
951  B(JS,JT)=C(JS,JT)
IV=MB 2
CALL INV (A,B,C,MB,MB,IV,LAL,LBL,MBL,D  )
DO 914 JO=1,MB
DO 914 JP=1,MB
914  A(JO,JP)=B(JO,JP)
DO 956 JU=1,LB
956  B(JU,1)=F(JU)
LZ=LB+1
CALL MULT(E,B,C,MB,1,LZ,LAL,LBL,MBL  )
DO 960 JV=1,MB
960  B(JV,1)=C(JV,1)
CALL MULT(A,B,C,MB,1,MB,LAL,LBL,MBL  )
WRITE(5,111)
111  FORMAT(1H1,42X, THE SOLUTIONS TO THE SYSTEMS OF EQUATIONS ARE  )

```

C.....WRITING OUT THE SOLUTIONS TO THE SYSTEM OF EQUATIONS.

200 DO 107 MD=1,MB

AV=AV+(C(MD,1)) 2

107 WRITE(5,106) MD, C(MD,1)

106 FORMAT(58X, 1HY, I2, 1H=.E16.)

AV=(AV) .5

WRITE(5,260) AV

260 FORMAT(////, 4X, 21H THE VECTOR IS. R=.E16.6, ////)

RETURN

END

REFERENCES

1. Bassett, C. A. L., "Biological Significance of Piezoelectricity," *Calcified Tissue Research*, Vol. I, 1968, p 252-272.
2. Bassett, C. A. L., "Electrical Effects in Bone," *Scientific American*, Vol. CCXIII, Oct., 1965, p 23.
3. Reference 1, p 263.
4. Fukada, E. and I. Yasuda, "Piezoelectric Effects in Collagen," *Japanese Journal of Applied Physics*, Vol. III, Feb., 1964, p 117-121.
5. Williams, W. S., "Piezoelectricity in Tendon and Bone," Dept. of Physics and Materials Research Laboratory, U. of Ill., p 5.
6. Gjelsvik, B., "Bone Remodeling and Piezoelectricity-II," *Journal of Biomechanics*, Vol. VI, 1973, p 187.
7. Reference 5, p 16.
8. Reference 4, p 120-121.
9. Stroke, G. W., *An Introduction to Coherent Optics and Holography*, Academic Press, New York, N. Y., 1969, p 209-210.
10. Smith, H. M., *Principles of Holography*, John Wiley and Sons, Inc., New York, N. Y., 1969, p 11.
11. Collier, R. J., C. B. Burckhardt, and L. H. Lin, *Optical Holography*, Academic Press, New York, N. Y., 1971, p 423-426.
12. Aleksandrov, E. B. and A. M. Bonch-Bruevich, "Investigations of Surface Strains by the Hologram Technique," *Soviet Physics-Technical Physics*, Vol. XII, no. 2, Aug., 1967, p 258-265.

13. Reference 11, p 426-431.
14. Reference 11, p 431-436.
15. Searle, S. R., Matrix Algebra for the Biological Sciences, John Wiley and Sons, Inc., New York, N. Y., 1966, p 227-228.
16. Melissinos, A. C., Experiments in Modern Physics, Academic Press, New York, N. Y., 1966, p 462-463.
17. Noble, B., Applied Linear Algebra, Prentice-Hall, Inc., New Jersey, 1969, p 40-41.